Modelling of liquid metal stirring induced by four counter-rotating permanent magnets

Dzelme, V.; Scepanskis, M.; Geza, V.; Jakovics, A.; Sarma, M.;

Originally published:

December 2016

Magnetohydrodynamics 52(2016)4, 461-470

Perma-Link to Publication Repository of HZDR:

https://www.hzdr.de/publications/Publ-24988

Modeling of liquid metal stirring induced by four counter-rotating permanent magnets

V. Dzelme[1], M. Ščepanskis[1], V. Geža[1], A. Jakovičs[1], M. Sarma[2]

[1] *Laboratory for Mathematical Modelling of Environmental and Technological Processes, University of Latvia, Zellu street 25, Riga, LV-1002, Latvia*

[2] *Institute of Fluid Dynamics, Helmholtz-Zentrum Dresden-Rossendorf, P.O. Box 510119, 01314 Dresden, Germany*

In this work, we investigate numerically the stirring of liquid gallium in a rectangular crucible induced by four counter-rotating permanent magnets. Mean velocity and turbulence kinetic energy for different distances of the magnets from liquid metal vessel and magnet rotation speed is investigated. The flow is modeled using two turbulence models – Detached Eddy Simulation (DES) and k-ω Shear Stress Transport (SST) and compared with experimental results obtained using the Dynamic Neutron Radiography Method. Numerical results show qualitative agreement with the experiment. Simulation results show that k-ω SST and DES turbulence models predict velocity and turbulence kinetic energy equally well. It is also shown that, in this system, characteristic turbulence kinetic energy is proportional to the square of characteristic velocity magnitude.

Introduction

Electromagnetic (EM) methods for liquid metal stirring, mixing and pumping are successfully used in industry [1,2,3]. In traditional AC inductors stirring efficiency is low, because to produce Lorentz force large enough to effectively drive the flow requires strong current in the coil. Permanent magnet stirrers have advantages in this regard – simpler design (no coil windings), smaller size and weight and high induced Lorentz force can be easily achieved [3,4].

Melt stirring efficiency is described by the velocity and turbulence intensity in the flow. Limiting factor of permanent magnet systems is melt temperature. To use permanent magnets in system with high temperature (above 500ºC), thick walls separating magnets from the melt must be used, decreasing magnetic field in the melt and consequently stirring and mixing efficiency.

There are many methods for liquid metal flow investigation, for example, Ultrasonic Doppler Velocimetry [5], potential difference probe [6], numerical modelling [7] and others. Recently, the first neutron radiography experiment for liquid metal flow visualization was reported in [8].

Numerical modelling is a powerful tool for flow investigation, but requires experimental validation. Nearly all flows of industrial interest are turbulent, therefore turbulence modelling must be applied. For industrial flows, Reynolds Averaged Navier-Stokes (RANS) turbulence models are usually employed, because these models are relatively cheap (compared to Large Eddy Simulation (LES) and Direct Numerical Simulation (DNS)). With ever-increasing computer capabilities, LES is also finding its way in industrial flow modelling. There also exist hybrid turbulence models – Detached Eddy Simulation (DES), which combine RANS (near walls, boundary layers) and LES (away from walls, free stream), which offer a compromise between accuracy and calculation time.

In this work, we investigate numerically liquid gallium flow in a rectangular crucible induced by four counter-rotating permanent magnets and compare the results to the data from the neutron radiography experiment [12]. We employ RANS and DES turbulence models and analyze time-averaged velocity and turbulence kinetic energy distributions in dependence on the permanent magnet distance from the melt and rotation frequency. Here, turbulence kinetic energy includes all velocity deviations from time-averaged velocity distribution, i.e. both large scale vortical transitions and small scale fluctuations.

System description

The system consists of a rectangular vessel filled with liquid gallium (temperature T = 30°C, density ρ = 6080 kg/m^3, viscosity μ = 1.97 mPa·s, electric conductivity $\sigma = 3.7 \cdot 10^6$ S/m [13]) and four counter-rotating cylindrical permanent magnets (remanence B_r = 1.3 T) located next to the vessel along the smallest dimension. Scheme of the active part of the system is shown in Fig. 1, coordinate system origin is in the center of the melt. The same system was investigated in [8 – 11].

The flow in this system is highly turbulent and unstable (Reynolds number ~10^5). The symmetrical four-vortex structure transits to three-eddy structure with third, diagonal vortex changing direction [11], but the time averaged pattern is symmetrical.

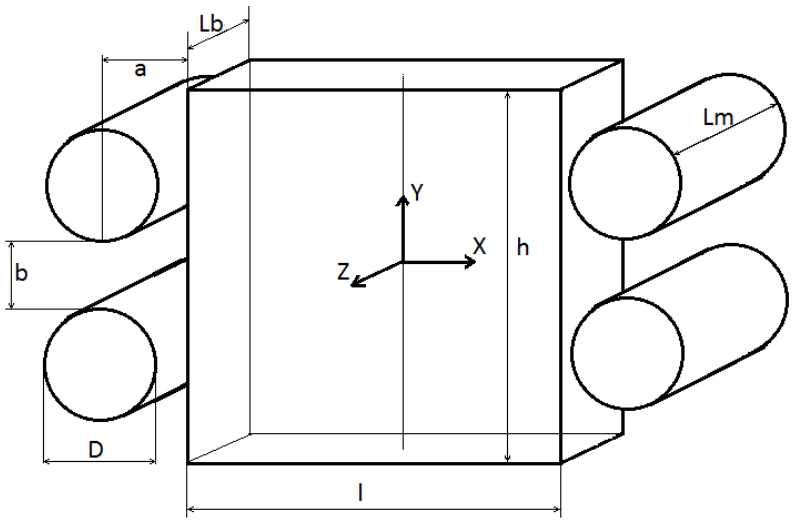

Fig. 1. Scheme of the permanent magnet stirrer.

Fixed system sizes are listed in Table 1. Permanent magnet distances *a* and corresponding rotation frequencies *f* used in this work are summarized in Table 2.

Table 1. Fixed system sizes.

h	100 mm
l	100 mm
D	15 mm
Lm	50 mm
Lb	30 mm
b	50 mm

Table 2. Combinations of magnet distances and rotation frequencies.

a, mm	f, Hz
21	21.15
25	21.15
25	40.00
40	21.15
40	10.00

Modeling

The numerical procedure consists of two parts. First, 3D electromagnetic simulation is performed to obtain the Lorentz force density distribution. Next, the force is included in fluid flow simulations as a momentum source.

Now, the electromagnetic force density in this system depends on the fluid velocity – the induced force depends on the relative motion of the magnets and the fluid. Therefore, to obtain correct electromagnetic force density distribution, it is necessary to take into account fluid velocity or, in other words, solve the electromagnetic problem in fluid element frame of reference. It is accomplished by an iterative electromagnetic–hydrodynamic coupling. First, the Lorentz force distribution is calculated for fluid with zero velocity and averaged over one period of magnet rotation. Next, fluid dynamics simulation is performed using the averaged Lorentz force as a momentum source. The flow is averaged over 60 seconds to obtain symmetrical four-vortex velocity field. This is one coupling iteration. Following iterations are done exactly the same way, but now in EM simulation taking into account the time-averaged fluid velocity. Usually, only three coupling iterations are enough to obtain a converged Lorentz force.

During the coupling phase, EM calculations are done in ANSYS Classic and fluid dynamics – in OpenFOAM (custom made solver based on pisoFoam to include momentum source term is used). EM mesh consists of four magnets, melt and air domain around them, 189k elements in total and zero magnetic vector potential is applied to air domain exterior. The iterative algorithm is described in more detail in [10].

After a converged Lorentz force is acquired, it is then used to perform the final flow simulations. The final flow simulations are performed in OpenFOAM using DES and k-ω SST turbulence models, using time-averaged four-vortex structure as initial velocity distribution. The DES turbulence model used is Spalart-Allmaras Improved Delayed Detached Eddy Simulation (IDDES) [15]. For DES simulations, the mesh consists of 1.035M hexahedral elements and time step ranging from 0.4 ms to 1 ms (depends on maximum velocity). For k-ω SST model (also during the EM-HD coupling phase) mesh is 300k hexahedral elements and time step ranging from 0.5 ms to 2 ms. For all cases Gauss linear integration scheme for divergence and Laplacian terms and backward time integration is used, the boundary conditions are no-slip for all walls and the free surface is fixed.

Results and discussion

First of all, the electromagnetic results were verified by running simulations for different mesh resolutions. It was found that the result for mesh of 189k elements was mesh converged (with error below 10%). Therefore, the mesh of 189k elements was used for

further simulations. Typical EM force density distribution is shown in Fig.2. As expected, maximum force is near the magnets and directed in the direction of magnet rotation.

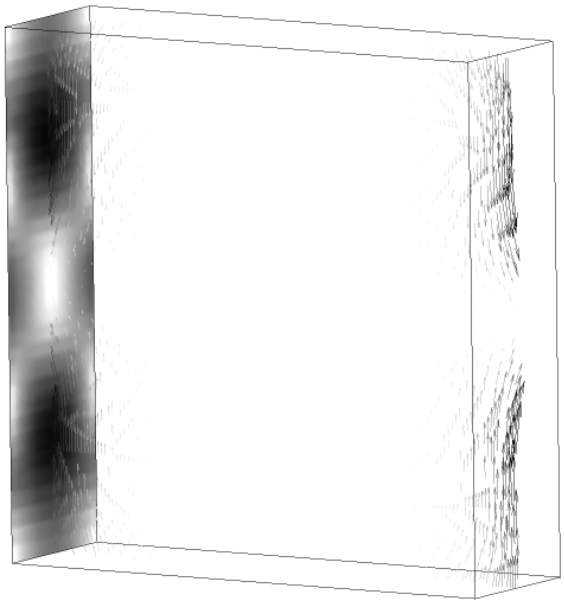

Fig. 2. Typical EM force density distribution – magnitude near wall and vector in middle plane, black – maximum, white – minimum.

Now, Figure 3 shows characteristic time-averaged velocity and turbulence kinetic energy distribution on vertical middle plane (Z = 0). Darker color corresponds to higher value. Clearly, maximum time averaged velocity is next to the magnets and maximum turbulence kinetic energy is located between the vortices. The locations of these mean maximum values are independent of magnet distance and rotation speed, but the values depend strongly on distance and speed.

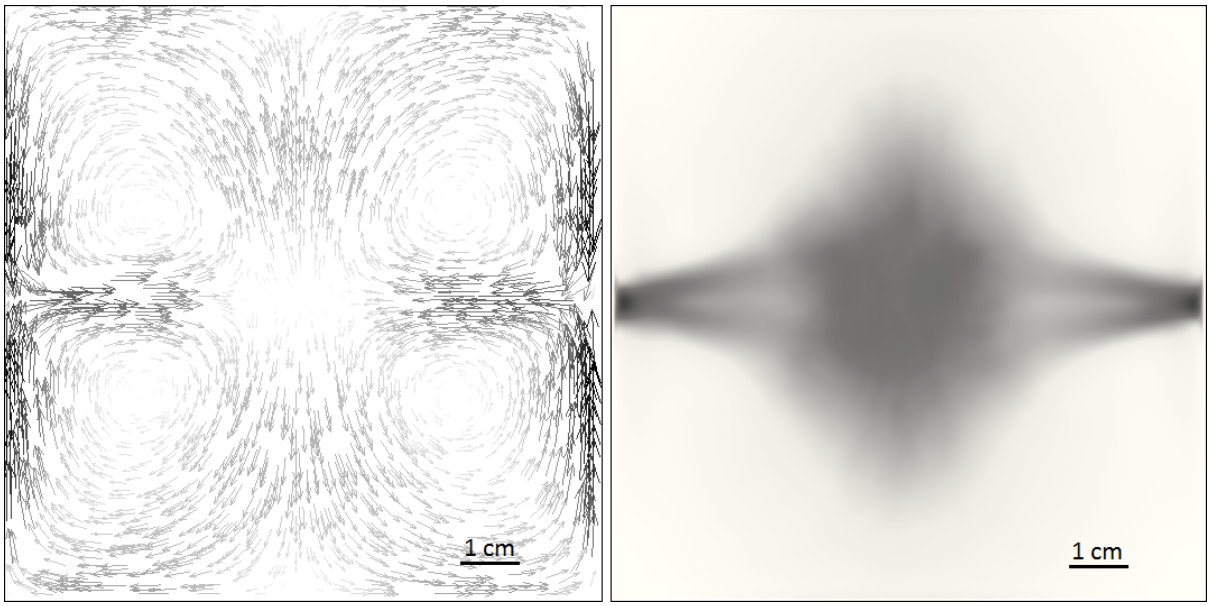

Fig. 3. Time-averaged velocity (left) and turbulence kinetic energy (right) on plane Z = 0

To verify our computational approach, several test simulations were performed for frequency f = 21.15 Hz and magnet distance a = 25 mm. To test how boundary condition on the free surface affects the results, we ran two simulations – one with no-slip and one with

free-slip condition on the upper wall of the melt (which correspods to the free surface). Also, we ran one test calculation with k-ω SST turbulence model on a finer mesh (1.035M elements). To verify our computation approach with OpenFOAM, one simulation was performed in commercial package ANSYS CFX. Test simulation results on a vertical line through the center of the vessel (between the vortices) are summarized in Figure 4. For the SST model the turbulence kinetic energy consists of resolved and modelled part, but for DES – only resolved part.

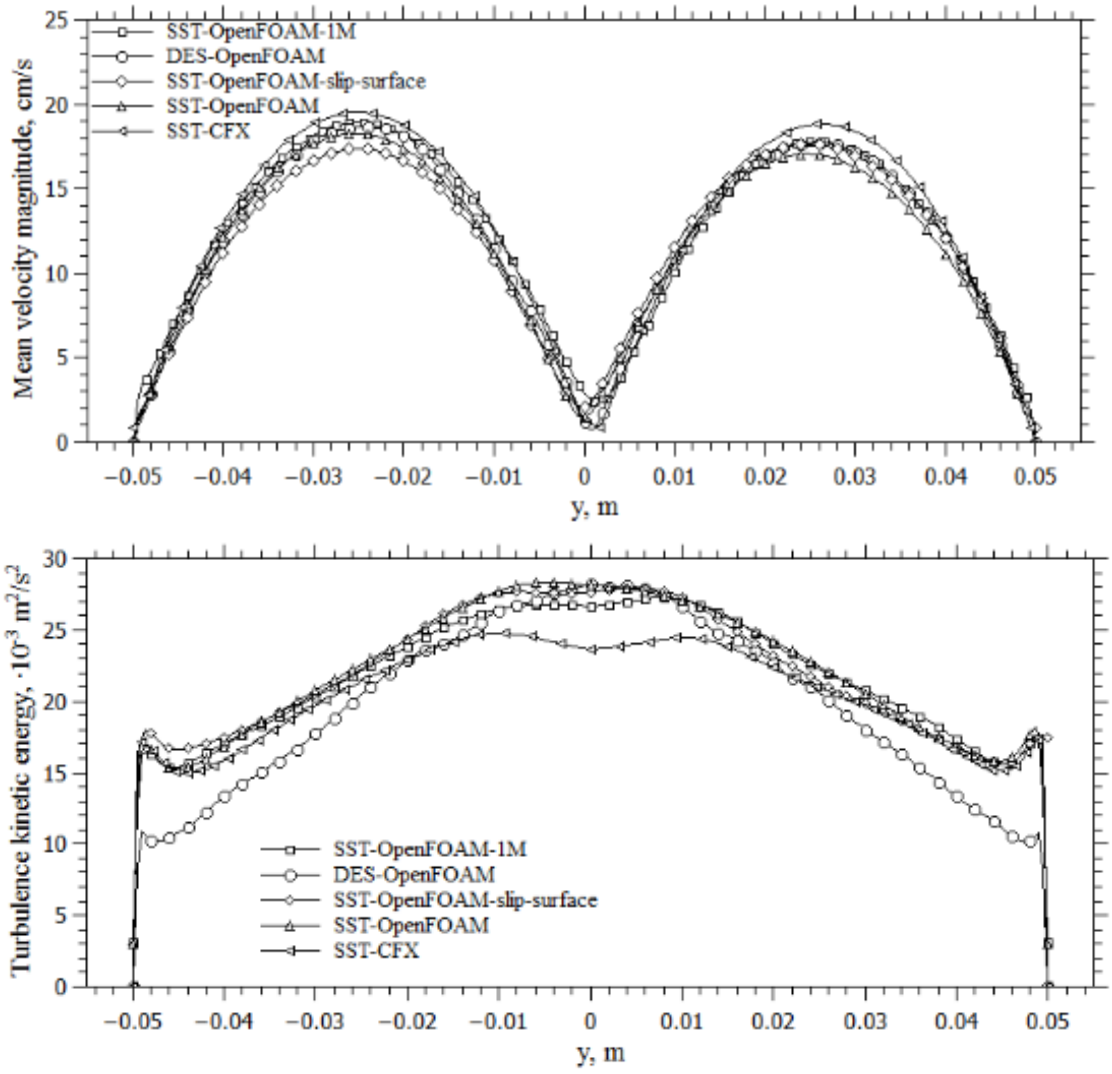

Fig. 4. Numerical verification results for magnet rotation frequency f = 21.15 Hz and distance a = 25 mm on a vertical line through the middle of the vessel, top – time-averaged velocity, bottom – turbulence kinetic energy.

Few things can be concluded from the test results shown in Fig. 4. Firstly, for k-ω SST model velocity and turbulence kinetic energy, in the considered range of mesh resolution, is independent of the mesh resolution. Secondly, the boundary condition for the free surface affects the results very little. Velocity and turbulence kinetic energy are very close for both cases (slip and no-slip conditions for the free surface), the only difference is near the surface – for the free-slip case velocity and turbulence kinetic energy doesn't go to zero at the surface, but for no-slip it does. Thirdly, the results of OpenFOAM and CFX are in a good agreement, increasing our confidence in OpenFOAM results.

Taking into account the test results, the rest of simulations were performed in OpenFOAM using only no-slip condition, 300k mesh elements for k-ω SST and 1.035M for DES.

For experimental validation, we present, in Figure 5, the results on a vertical line through the center of the vessel for magnet distance a = 21 mm and rotation frequency f = 21.15 Hz in comparison with the experiment. In experiment the magnet distance was (21 ± 3) mm. Currently, we have the neutron radiography experiment data only for this particular magnet distance and rotation frequency.

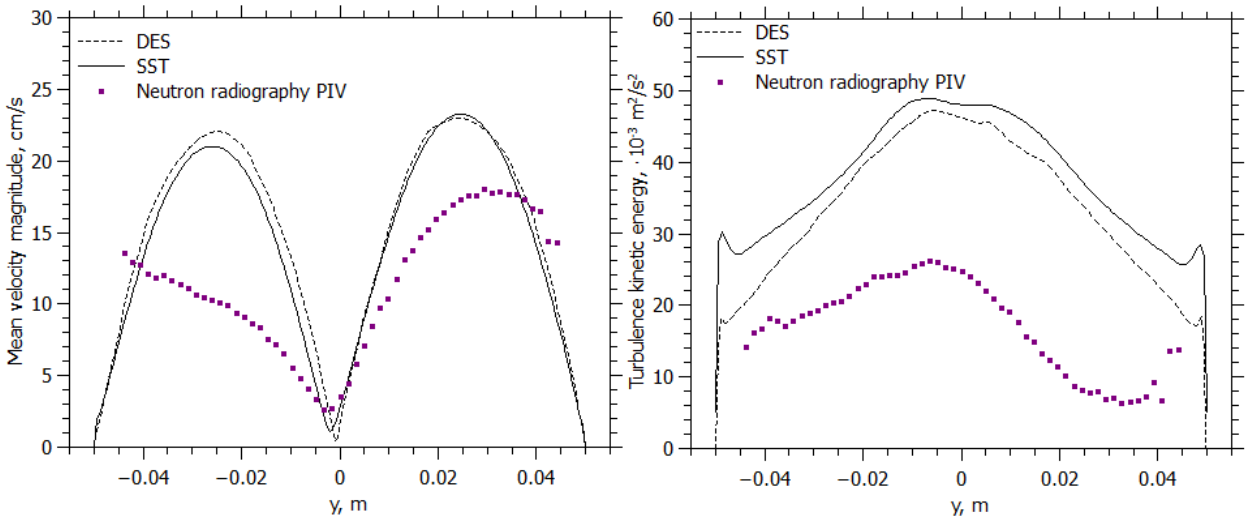

Fig. 5. Results for f = 21.15 Hz and magnet distance a = 21 mm on a vertical line through the middle of the vessel, left – time-averaged velocity, right – turbulence kinetic energy.

Simulation results show only qualitative agreement with the experiment. Reasons for quantitative disagreement can be various. Firstly, the uncertainty in the magnet distance in the experiment is 3 mm, which constitutes about 14% of 21 mm. Since the magnetic field decreases rapidly with increasing distance, the error in distance has an important effect on the induced EM force and, consequently, velocity and turbulence energy. Secondly, experimental data is two-dimensional (experimentally acquired are shadow images in the Z direction, therefore, velocity in this direction is not detected), but simulations – 3D. Therefore, experimental data for velocity and turbulence kinetic energy does not include Z component of velocity and velocity fluctuations, respectively. Also, time resolution in simulations is much better – time step ranges from 0.4 to 2 ms, but in experiment image acquisition rate is 32 frames per second (time step ~31 ms), therefore some fluctuations are damped out. Thirdly, the system is very sensitive to the vessel centering between the magnets [12]. This can lead to asymmetrical Lorentz force and, consequently, velocity and turbulence kinetic energy distribution. The centering problem also causes one specific direction of the diagonal vortex to dominate [11]. Finally, as it was also noted in [11], since the dynamic neutron radiography methodology is still new, more work is needed to improve the quality of the experiments and data analysis, and it should also be validated by other experimental methods (for example, UDV).

Now, to describe melt dynamics in the system, characteristic velocity and turbulence kinetic energy can be used. In this case, we choose maximum time-averaged velocity and volume average turbulence kinetic energy as the characteristic values. Since we are considering different magnet rotation frequencies and also distances from the melt, to describe a specific frequency/distance combination, we introduce a parameter:

$$F = afB^2 \tag{1}$$

where a – distance from magnet axis to the liquid metal, f – magnet rotation frequency, B – magnetic flux density magnitude that a single cylindrical permanent magnet with remanence B_r = 1.3 T would produce at a distance a from its axis in the direction of magnetization. For the considered range of frequency and magnet distance, the secondary (induced) magnetic field is small, therefore, it is not considered in the analysis. Since the induced electromagnetic force density is proportional to $f{\cdot}B^2$ [14], it is also proportioanl to the parameter F. Magnetic field B is calculated as follows [14]:

$$B = \frac{B_r}{2}\left(\frac{D}{2a}\right)^2 \tag{2}$$

where D – magnet diameter.

Numerically calculated characteristic values as functions of the parameter F are shown in Figure 6. Since, in the PIV analysis of the neutron shadow images, regions near walls are removed (particle concentration is too high) and velocity near walls is highest, experimental maximum velocity is highly underpredicted. Even though experimental volume average turbulence kinetic energy seems to be in a good agreement with simulation, it is actually overestimated, since regions of low fluctuations (near walls) are cut off in PIV analysis.

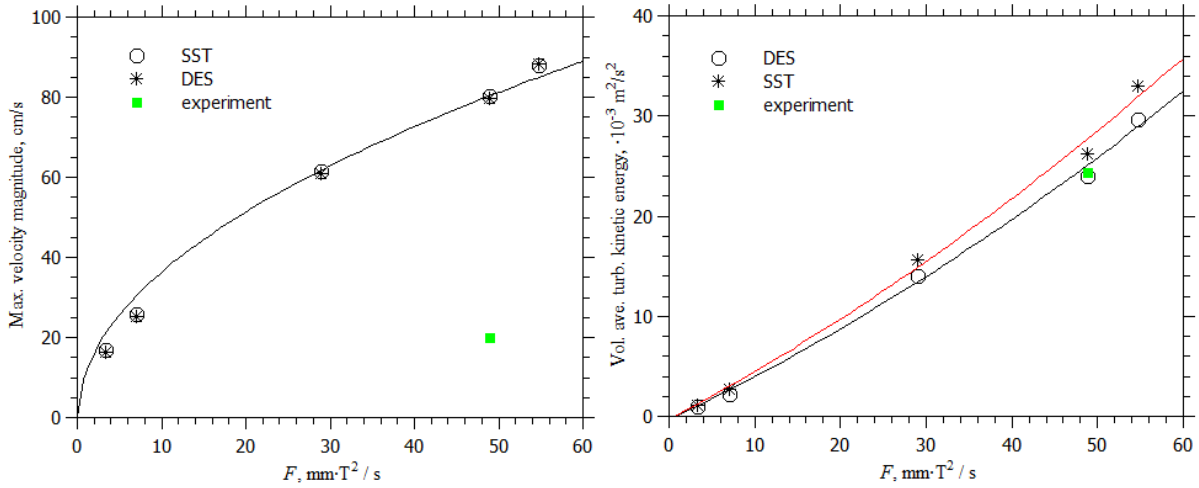

Fig. 6. Max. velocity (left) and volume average turbulence kinetic energy (right) as a function of F.

Clearly, velocity is proportional to $\sqrt{F}$ and turbulence kinetic energy is proportional to F^2. It means that, increasing induced force density, flow instabilities grow faster than mean velocity. Turbulence kinetic energy is proportional to the square of velocity, which is clearly demonstrated in Figure 9 (lines – second order polynomial fit).

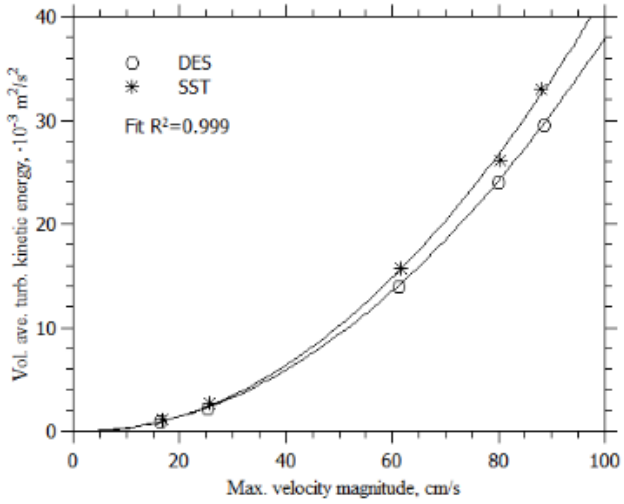

Fig. 7. Volume average turbulence kinetic energy as a function of max. velocity magnitude.

Now, considering the relationship shown in Fig. 6, we can estimate the influence of uncertainty in magnet distance on the results. In the neutron radiography experiment, the uncertainty in magnet distance was 3 mm. It is found that, increasing magnet distance by 3 mm, the maximum velocity can decrease by about 18% and average turbulence kinetic energy by about 38%. Therefore, it justifies our previous statement that the error in magnet distance from the melt determines a large part of the disagreement between the experiment and simulations (see Fig. 5 and the text below it).

Conclusions

Both k-ω SST and DES turbulence models are predicting time-averaged velocity equally well. For k-ω SST model, turbulence kinetic energy is the sum of resolved long term pulsations and modeled isotropic part, but for DES – only resolved, limited by time and space discretization. By correct discretization, the sub-grid viscosity modeled part of turbulence kinetic energy is small. Therefore, k-ω SST model predicts only slightly higher turbulence kinetic energy than the DES model.

In this work, two system parameters were varied – magnet distance from the melt a and rotation frequency f. To describe a specific magnet distance and frequency combination, parameter $F = afB^2$ was introduced. Simulation results show that the characteristic (in this case – maximum) mean velocity is proportional to $\sqrt{F}$. On the other hand, turbulence kinetic energy is proportional to F^2. Therefore, the parameter F, at least in the considered range of magnet distance and rotation frequency, allows us to estimate the characteristic velocity and turbulence level in the system.

Volume average turbulence kinetic energy, which is responsible for mixing efficiency, grows proportionally to the square of characteristic velocity. In other words, turbulence kinetic energy grows proportionally to the mean flow kinetic energy, which is as expected, since the turbulent pulsations gain energy from the mean flow.

The neutron radiography results show only qualitative agreement to the simulations. From the relationships shown in Figure 6, it was found that the quantitative disagreement between simulation and experiment is mostly due to the error in magnet distances to melt. Since the neutron radiography is still a new methodology, more work is necessary to improve it, including validation using other experimental methods, for example, UDV.

References

[1] A. Lehman, O. Sjoden, A. Kuchaev, Electromagnetic equipment for non-contacting treatment of liquid metal in metallurgical processes, *Magnetohydrodynamics, Vol. 42, 2006, pages 299-306*

[2] M. Kirpo, A. Jakovics, E. Baake, B. Nacke, Modeling velocity pulsations in a turbulent recirculated melt flow, *Magnetohydrodynamics, Vol. 42, 2006, pages 207-218*

[3] T. Beinerts, A. Bojarevics, I. Bucenieks, Y. Gelfgat, I. Kaldre, Use of permanent magnets in electromagnetic facilities for the treatment of aluminum alloys, *Metallurgical and Materials Transactions B, Vol. 47, Nr 3, 2016*

[4] I. Bucenieks, K. Kravalis, Efficiency of EM induction pumps with permanent magnets, *Magnetohydrodynamics, Vol. 47, 2011, pages 89-96*

[5] S. Eckert, G. Gerbeth, Velocity measurements in liquid sodium by means of ultrasound Doppler velocimetry, *Experiments in Fluids 32, 2002, pages 542–546*

[6] A. Cramer, K. Varshney, Th. Gundrum, G. Gerbeth, Experimental study on the sensitivity and accuracy of electric potential local flow measurements, *Flow Measurement and Instrumentation 17, 2006, pages 1–11*

[7] M. Kirpo, A. Jakovics, B. Nacke, E. Baake, M. Langejurgen, LES of heat and mass exchange in induction channel furnaces, *Przeglad Elektrotechniczny, R. 84 NR 11/2008, pages 154-158*

[8] M. Scepanskis, M. Sarma M, R. Nikoluskins, K. Thomsen, A. Jakovics, P. Vontobel, T. Beinerts, A. Bojarevics, E. Platacis, A report on the first neutron radiography experiment for dynamic visualization of solid particles in an intense liquid metal flow, *Magnetohydrodynamics, Vol. 51, 2015, pages 257-266*

[9] M. Sarma, M. Scepanskis, A. Jakovics, K. Thomsen, R. Nikoluskins, P. Vontobel, T. Beinerts, A. Bojarevics, E. Platacis, Neutron radiography visualization of solid particles in stirring liquid metal, *Physics Procedia, Volume 69, 2015, pages 457-463*

[10] M. Scepanskis, E. Yu. Koroteeva, V. Geza, A. Jakovics, Simulation of liquid metal flow induced by four counter rotating permanent magnets in a rectangular crucible, *Magnetohydrodynamics, Vol. 51, 2015, pages 37-44*

[11] V. Dzelme, M. Sarma, V. Geza, M. Scepanskis, A. Jakovics, Transition of different vortical structures in rotating permanent magnets agitated flow: numerical and experimental neutron radiography investigation, *10th PAMIR International Conference, June 20 – 24, 2016, Cagliari, Italy*

[12] M. Scepanskis, M. Sarma, P. Vontobel, P. Trtik, K. Thomsen, A. Jakovics, T. Beinerts, Assessment of electromagnetic stirrers agitated liquid metal flows by dynamic neutron radiography, *Metallurgical and Materials Transactions B,* (submitted)

[13] N. B. Morley, J. Burris, L. C. Cadwallader, M. D. Nornberg, GaInSn usage in the research laboratory, *Review of scientific instruments 79, 2008*

[14] A. Bojarevics, T. Beinerts, Experiments on liquid metal flow induced by a rotating magnetic dipole, *Magnetohydrodynamics, Vol. 46, 2010, pages 333-338*

[15] M. Shur, P. Spalart, M. Strelets, A. Travin, A hybrid RANS-LES approach with delayed-DES and wall-modelled LES capabilities, *International Journal of Heat and Fluid Flow 29, 2008, pages 1638–1649*